Comparative Study of Different Parameter Inversion Methods

Jiangtao Quan, Keji Chen, Jing Xu, Xishan Wen, Zhuohong Pan, Qi Yang

Abstract—**In order to obtain the objective function for four point method, the theoretical expression of objective function and its partial derivative have been obtained and computed by complex image method , which satisfies all the need of traditional optimal methods of direct search and gradient-based. The traditional optimal methods have been used as the inversion method of earth parameter on inversed error, iterative number and CPU time. Most of these method are trapped into local solution because the earth parameter inversion is a highly nonlinear problem. The least square method and trust region method are the better methods for earth parameter inversion for their performance on accuracy and numerical stability. To improve the consistance of the inversed results, the least square method and trust region method with constrained conditions have been proposed. The constrained inversion with weights can normalize the resistivity and reflect the upper and deeper soil parameters, so the least square method with constrains and weights is recommend as the earth parameter inversed method of grounding grid design. In order to obtain the apparent resistivity curve precisely, the general configuration of pole distance is recommended to increase by 1:1.5 for the adjacent pole distance.**

Index Terms—**four-point method, earth parameters estimation, horizontal multilayer soils (HMS), probe spacing configuration.**

I. INTRODUCTION

Earth parameter which determines grounding impedance and step/touch potential, is an essential part of grounding grid design[1], [2].In the real geological formation, electrical conductivity distribution of earth is inhomogeneous. So earth parameters estimation (EPE) is aim for acquisition and utilization of the earth structure and composition by practical measured data.

The models of earth parameter have been more sophisticated, other than the spherical model [3], cylindrical form [4] and finite volume structure [5], horizontal multilayer earth(HME) are more widely used to simulate the real soil in grounding design [6], [7]. EPE is an optimization problem of apparent resistivities measured by four-point methods [8].

Based on complex image method, the measured apparent resistivity by Wenner arrangement is interpreted by BFGS quasi−Newton method [9]. As partial derivatives of apparent resistivities according to earth parameters have been derived, this method is more efficient than classical image method.

Recently, generic algorithm (GA) has been applied in soil parameter estimation to increases the accuracy in the calculation of parameters of horizontal multilayer earth. The error comparison between J. Alamo [10] and GA by I. F. Gonos [10] showed that J. Alamo's methods for parameters estimation of two-layer earth is with considerably higher error when compared with GA methodology. Based on Sunde's algorithm [11] and GA, W. P. Calixto [12] presented a better estimation method considering the number of layers. Moreover, W. P. Calixto used the 3−D soil stratification methodology to increase the resolution of electrical properties of the local soil model [13].

In early researches, HMS with two layers has been well developed [14], [15]. For three-layer earth interpretation, the electrostatic images generating method (EIG) for HMS [16], [17]. It is time-consuming during iterative computation process. But In fact, the EIG can be mathematically derived using Taylor's expansion of Green's function of HMS [6].Due to the limitation of implementation efficiency, EIG is not widely used in soil parameter inversion (SPI) of HMS which is more than 3 layers. As an improvement of EIG, complex image method (CIM) has been introduced to carry out calculation of Green's function of HMS [6]. Moreover, for SPI of HMS, BFGS quasi−Newton method has been put forwards by CIM solution of Green's function and its derivatives to earth parameters [9]. But for all the gradient−base methods, the derivation methods for HMS are rather complicated when n>4 [6], [9]. If $n > 3$, optimization methods converge to local optima easily which may lead to considerable larger error than global optima or real situation. As a derivative free method, GA is time−consuming and local−minimum−convergent in some cases. Even with GA, traditional method [18] and Sunde's algorithm [16] have produced different results by [10], [12].

Although a lot of research conducted, comprehensive com parison of various methods' performance haven't been done, and the problems of pole layout principle and the difference of the inversion results have not been effective study, which must be further discussed.

Based on the objective function of horizontal multilayer s oil parameters inversion and combing with the example, this article compares the performance of different methods, and a

Manuscript received June 10, 2014; revised August 7, 2014.

Jiangtao Quan is with the Key Laboratory of High-Voltage Field-test Technique of Electric Power Research Institute of Hubei Power Grid Corporation, Wuhan, CO 430077 China(e-mail: quanjtao@163.com).

Keji Chen is with the Huizhou Power Supply Company, Yichang, CO 443000 China. (e-mail: 13972020739@139.com).

Jing Xu is with the Huizhou Power Supply Company, Yichang, CO 443000 China. (e-mail: xujing@163.com).

Xishan Wen is a Professor and Doctoral Supervisor at Wuhan University, Wuhan, CO 430072 China (e-mail: xswen@whu.edu.cn).

Zhuohong Pan is a visiting scholar at the University of Tennessee, Knoxville (e-mail:leekey2@163.com).

Qi Yang is a postgraduate from Wuhan University, CO 430072 China (e-mail: whu_yangqi@qq.com).

nalyzes the effect of polar distance on soil parameter measur ement, also this article summarizes the pole layout principle. And to solve the problem of exotic and different inversion r esults, soil parameter inversion method with constraints was proposed, and is verified by an example.

II. OBJECTIVEFUNCTION OF SOIL PARAMETERS INVERSION OF HORIZOTAL MULTILAYER SOILS

As shown in Fig.1, scalar potential ϕ of an arbitrary observation point satisfies Poison's equation in the cylindrical coordinate:

$$\frac{\partial^2\phi}{\partial r^2}+\frac{1}{r}\frac{\partial\phi}{\partial r}+\frac{\partial^2\phi}{\partial z^2}=-\rho_1 I\delta(d),\ r=\sqrt{x^2+y^2} \quad (1)$$

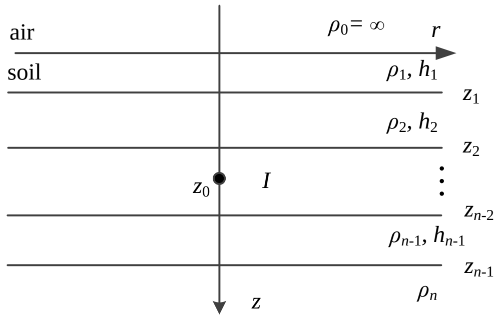

Fig.1. horizontal n-layer soil. ρ_j and h_j is resistivity and thickness of layer j. z_j is z-axis coordinate of boundary of layer j and layer j+1, j=1,2,…,n−1.

Where δ is referred to as the Dirac delta function and d is denoted by distance between the observation point and the point current source. The closed form of ϕ can be written as

$$\phi_i(x,y,z,z_0)=\frac{\rho_i I}{4\pi}\int_0^{+\infty}\left[A_i e^{-\lambda(z-z_0)}+B_i e^{\lambda(z+z_0)}\right]\mathrm{J}_0\left(\lambda\sqrt{x^2+y^2}\right)\mathrm{d}\lambda \quad (2)$$

Where ϕ_i is the scalar potential of layer i, λ is the integral variable and J_0 is zero order Bessel function of first kind. A_i and B_i can be theoretically derived and then approximated by complex image method:

$$A_i(\lambda)=\sum_{j=1}^{N_{Ai}}\alpha_j e^{\beta_j\lambda},\ B_i(\lambda)=\sum_{j=N_{Ai}+1}^{N_{Ai}+N_{Bi}}\alpha_j e^{-\beta_j\lambda} \quad (3)$$

Where N_{Ai} and N_{Bi} is the number of complex images of A_i and B_i, α and β is the amplitude and location of the complex image (3) into (2) gives

$$\phi_i(x,y,z,z_0)=\frac{\rho_i I}{4\pi}\sum_{j=N_{Ai}+1}^{N_{Ai}+N_{Bi}}\frac{\alpha_j}{\sqrt{x^2+y^2+\left(z-z_0-\beta_j\right)^2}},\ i=1,\cdots,n \quad (4)$$

For the four−point configuration shown in Fig.2, the voltage difference of the potential probes is given by:

$$\begin{aligned}V_{P1}-V_{P2}=&\phi_{P1}\left(x_{C1}-x_{P1},y_{C1}-y_{P1},z_{P1},z_{C1}\right)\\&-\phi_{P1}\left(x_{C2}-x_{P1},y_{C2}-y_{P1},z_{P1},z_{C2}\right)\\&-\phi_{P2}\left(x_{C1}-x_{P2},y_{C1}-y_{P2},z_{P2},z_{C1}\right)\\&+\phi_{P2}\left(x_{C2}-x_{P1},y_{C2}-y_{P1},z_{P1},z_{C2}\right)\end{aligned} \quad (5)$$

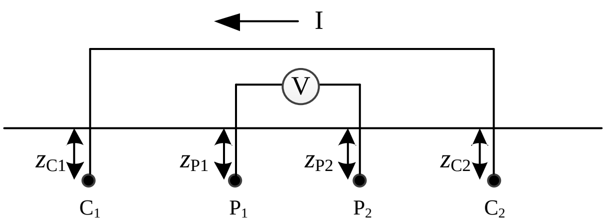

Fig.2. configuration of four–point method.

Potential difference of P_1 and P_2 can be written as

$$V_{P1}-V_{P2}=\frac{\rho_a I}{4\pi}\left(D_{C1-P2}+D_{C3-P4}-D_{C1-P3}-D_{C2-P4}\right) \quad (6)$$

where ρ_a is the apparent resistivity. D_{A-B} is defined as

$$D_{P-Q}=\frac{1}{\sqrt{\left(x_P-x_Q\right)^2+\left(y_P-y_Q\right)^2+\left(z_P-z_Q\right)^2}}+\frac{1}{\sqrt{\left(x_P-x_Q\right)^2+\left(y_P-y_Q\right)^2+\left(z_P+z_Q\right)^2}} \quad (7)$$

By definition of apparent resistivity, we have

$$\rho_a=\frac{4\pi\left(V_{P1}-V_{P2}\right)}{I\left(D_{C1-P2}+D_{C3-P4}-D_{C1-P3}-D_{C2-P4}\right)} \quad (8)$$

The objective function of parameter estimation is expressed as the root-mean-square (RMS) error

$$\min f_{RMS-error}\left(\rho_1,\cdots,\rho_n,h_1,\cdots,h_{n-1}\right)=\sqrt{\frac{\sum_{i=1}^{m}\left(\frac{\rho_{ai}-\rho_{Mi}}{\rho_{Mi}}\right)^2}{m}} \quad (9)$$

where ρ_{ai} and ρ_{Mi} is the apparent resistivity and measured resistivity respectively.

EPE belongs to small scale nonlinear optimization problem. It indicates that nonlinearity of SPI renders most optimized methods inefficient and stuck in the local optimum solutions. Moreover, choosing proper initial solution is important for the final solution in SPI. So, we will consider examples from each class, since no one method or class of methods can be expected to uniformly solve all problems with equal efficiency. Clearly it behooves the engineer to tailor the method used to inverse the parameters of HMS by the measured data at hand.

As shown in Fig.1, parameters of HMS, such as the number of layers (n), resistivity (ρ_i),thickness (h_i) and depth (z_i) of the i^{th} layer, can be obtained by processing measurement data with optimization methods.

III. INTRODUCTION OF METHODS FOR SPI

In next section, several comparative studies were surveyed and the selected results from a few of computational cases of SPI have been given, since painfully little of what is currently known of the performance of these methods on practical SPI problems has purely come from considerations of J. Alamo [19].

These methods of SPI were examined from primarily three perspectives: First, some methods are included because of their historical importance such as steepest decent method. Second, numerous methods were thought to be of practical importance in SPI like Genericalgorithm, BFGS quasi–Newton method and Levenberg–Marquardt method. Third, some new methods are available for application in SPI, such as simplex method[20] and trust region method. As these methods were discussed, we include to the extent possible, remarks that delimit advantages and disadvantages of those methods. It is, of course, nearly impossible to be complete in this effort, and in addition we have to avoid extensive discussion of rate and region of convergence.

For comparison of these methods, CDEGS, the commercial grounding computation software using SD and LM [21], and other research papers like BFGS [9], GA [10], [12] were

ISBN: 978-988-19252-0-6
ISSN: 2078-0958 (Print); ISSN: 2078-0966 (Online)

introduced. The methods introduced in this section are direct–search and gradient–based methods. Direct−search methods include:

1. Nelder–Mead simplex method (NM in IMSL and MATLAB);
2. Genetic algorithm (GA in MATLAB).

Gradient–based methods include:

1. Steepest decent method (SD in CDEGS);
2. Levenberg–Marquardtmethod (CLM in CDEGS, LM in IMSL and MATLAB);
3. Conjugate gradient method (CG in IMSL and MATLAB);
4. BFGS quasi–Newton methods (BFGS in IMSL and MATLAB);
5. Trust regions method (TR in MKL and MATLAB).

As the operational platforms of IMSL, MKL, MATLAB are different, the computation code has implemented by FORTRAN, C++ and MATLAB respectively.

The measured apparent riesistivities was shown in Table I. Table II shows that the result in [9] of 6-layer soil has 0.4% larger RMS error than 4-layer soil by using the same BFGS method. Moreover, the data in Table II have only 9 points which is inadequate for the inversion of 6-layer earth with 11 parameters. Even with 4-layer earth and the similar RMS error shown in Table III, variance of results shown in Table III with dispersion has been obtained by different approaches. In Table III, parameters of the top three layers are quite different but the very nearly the same resistivity of last layer was obtained. Because potential gradient of earth surface near grounding electrodes is mainly affected by top layer soil resistivity, a more stable inversed result is required to obtain a more likely explanation of top layer resistivity. The comparison of RMS errors of inversions and numbers of iterations was list in Table IV.

For the RMS error, we have LM≈ TR≈ CG≈ BFGS < NM < SD, and for the computational effort, we have TR, LM < SD,CLM < BFGS < CG < NM.

In earth parameters optimization problems, the variables involved are almost always subject to certain constrains, like the thickness cannot be too thin or too thick and the resistivity should be a normal value. The abnormal resistivity maybe unusually low (≤10Ω·m) or unusually high (≥10000Ω·m) [1]. In Table II, some singular results were produced, just like the parameter of 3rd layer solved by TR is 0.9Ω·m/0.1m. The presented methods used in this paper just try to get a better result in the searching space ignoring some considerations of the inversed parameters, and some results of unusual pattern could be found. So it's necessary to assign some additional constrains to the parameter inversion of HMS to obtain reasonable results avoiding the established search mode by the optimization methods. The method of SPI of HMS with constrains will be expressed in the next section.

For the gradient–based methods, LM and TR are superior to other methods for the numerical stability and convergent rate.

Table I

APPARENTRIESISTIVITIE, CASEII (BFGS [9])

a(m)	1	2	3	4	6	10	12	14	20
ρ_a(Ω·m)	74.5	84.6	78.6	66.9	50.9	55.3	54.3	56.3	61.6

Table II

INVERSED PARAMETERS OF BY [9],n= 6, RMS error: 3.1%

i	1	2	3	4	5	6
ρ_i(Ω·m)	68.0	627.9	7.3	387.3	7.0	125.4
h_i(m)	1.1	0.3	1.2	2.6	3.2	∞

Table III

COMPARISON OF THE RESULT BY DIFFERENT METHODS (n = 4)

RMS error	ρ_1(Ω·m)/ h_1(m)	ρ_2(Ω·m)/ h_2(m)	ρ_3(Ω·m)/ h_3(m)	ρ_4(Ω·m)
TR: 2.7%	32.6/0.9	206.5/1.1	0.9/0.1	72.4
BFGS: 2.7%	31.8/0.4	200.9/1.1	10.2/1.0	72.4
LM: 2.7%	28.5/0.3	318.4/0.7	5.7/0.6	72.1
CG: 2.7%	37.2/0.4	202.7/1.1	5.4/0.6	72.7
NM: 3.2%	64.3/0.9	383.9/0.4	24.1/2.8	73.2
SD: 3.5%	70.0/1.0	188.7/0.9	15.3/1.7	74.0

TABLE IV

COMPARISON OF DIFFERENT METHODS

method	NM	SD	CLM	LM	CG	BFGS	TR
RMS error (%)	3.2	3.5	2.7	2.7	2.7	2.7	2.7
number of iterations	980	119	507	106	414	64	39
CPU time (s)	8	2	2	1	4	3	1

IV. PROBE SPACING CONFIGURATION

The standard ρ−a curves of two layer earth have been detailed discussed in IEEE Std. 81–2012 [1]. However, the real ρ−a curves differ from the typical two layer case because the earth parameters are more complex and a standard probe spacing configuration should be proposed to meet the requirements of various earth structures. In order to sample the ρ−a curve by measuring apparent resistivities effectively and precisely, the proper ratio of probe spacing arranged in ascending order can be 1:1.5 approximately to get dense enough measured points. For example, the probe spacing can be set to 1m, 1.4m, 2m, 3m, 5m, 7m, 10m, 14m, 20m, 30m, 50m, 70m, 100m, …, a_{max}. The maximum spacing a_{max} could be 1~3 times as the diagonal length of the grounding grid in order to get the apparent resistivity of deep earth.

An example of the measured data by proposed probe spacing configuration and the ρ−a curve of a singular parameter 7-layer horizontal multilayer earth were shown in Fig. 7.The result showed that the presented probe spacing configuration can learn the detailed ρ−a curve and sample the curve precisely under unusual earth parameters. Moreover, the proposed probe spacing configurations a versatile method for all kinds of horizontal multilayer earths.

Actually, the unusually high or low resistivity layer can effectively screen the deeper layer while four−point method is applied. In Fig.3, it takes 1km as maximum probe spacing to obtain the detailed ρ−a curve of the test soil..

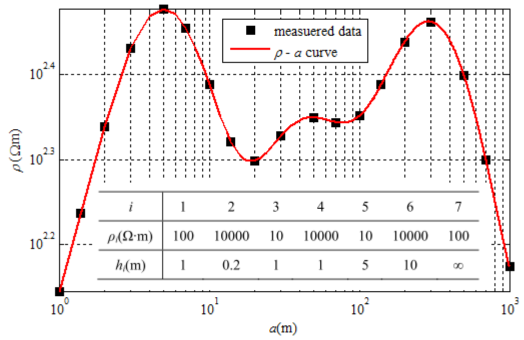

Fig.3.Theρ−a curve and measured resistivities of Wenner method using the proposed probe spacing configuration.

ISBN: 978-988-19252-0-6
ISSN: 2078-0958 (Print); ISSN: 2078-0966 (Online)

V. SOIL PARAMETERS INVERSION WITH CONSTRAINTS

Soil parameters inversion with constraints (SPIC) is aim for two aspects: 1) Avoiding unreasonable results such as unusual high/low resistivities and abnormal thick/thin layers. 2) Improving confidence for the resistivity of the top and deep soil, and preventing significant estimated bias of inversed resistivity to ensure the potential gradient of earth surface and grounding impedance in a reasonable range.

By introducing lower/upper bounds of earth parameters and the inequalities constrains of ratio of adjacent resistivities, the objective function of SPIC is defined as

$$\min f_{RMS-error}\left(\rho_1,\cdots,\rho_n,h_1,\cdots,h_{n-1}\right)=\sqrt{\frac{\sum_{i=1}^{m}\left(\frac{\rho_{ai}-\rho_{Mi}}{\rho_{Mi}}\right)^2}{m}} \quad (10)$$

Subject to:

$$\rho_{li}\le\rho_i\le\rho_{ui}, i=1,\cdots,n \quad (11)$$

$$h_{li}\le h_i\le h_{ui}, i=1,\cdots,n-1 \quad (12)$$

$$l_i\le\frac{\rho_i}{\rho_{i+1}}\le u_i, i=1,\cdots,n-1 \quad (13)$$

Where ρ_{li}, ρ_{ui}, h_{li}, h_{ui}, l_i and u_i are the lower and upper bounds of the resistivity, thickness and resistivity ratio of*i*th−layer respectively. ρ_{li}, ρ_{ui}, h_{li}, h_{ui} can be defined by the user.

For example, SPIC for Table I can be with the following lower/upper bounds and inequalities linear constraints

$$\begin{gathered}0.9\rho_{M1}\le\rho_1\le1.1\rho_{M1}, 0.8\rho_{M9}\le\rho_4\le1.25\rho_{M9}\\0.1\min\left(\rho_M\right)\le\rho_i\le10\max\left(\rho_M\right), i=2,3\\0.1\min\left(a\right)\le h_i\le\max\left(a\right), i=1,\cdots,3\\0.2\le\frac{\rho_i}{\rho_{i+1}}\le5, i=1,\cdots,3\end{gathered} \quad (14)$$

LM with lower/upper bounds and inequality constraints is proposed for SPIC. SPIC result of Table I was shown in Table V.

Another method to cope with this situation is introducing weighting coefficients ***w*** in the RMS error function:

$$\min f_{weight}\left(\rho_1,\cdots,\rho_n,h_1,\cdots,h_{n-1}\right)=\sqrt{\frac{\sum_{i=1}^{m}\left(\frac{\rho_{ai}-\rho_{Mi}}{\rho_{Mi}}w_i\right)^2}{m}} \quad (15)$$

$$\text{Subject to: } 0.2\le\frac{\rho_i}{\rho_{i+1}}\le5, i=1,\cdots,n-1.$$

For the importance of top and deep earth resistivity, *w* can be

$$w_i=\left|i-0.5m\right|+0.1-0.5\bmod\left(m,2\right), i=1,\cdots,m \quad (16)$$

The results of LM and TR for SPIC with weighting coefficients constraints (SPICW) were shown in Table V and Fig.4.

Table V shows, though RMS error is slightly larger than previous case, the difference of resistivity between adjacent layers has been controlled. By SPICW, the apparent resistivity curve at the top and deep layer region is closed to the measured data. So SPICW is recommended as it can get more precisely deep earth resistivity and grounding impedance [1] and the performance of LM on SPICW is superior to TR.

TABLE V
COMPARISON OF THE RESULT BY SPIC and SPICW (Table III, *n* = 4)

RMS error	ρ_1(Ω·m)/ h_1(m)	ρ_2(Ω·m)/ h_2(m)	ρ_3(Ω·m)/ h_3(m)	ρ_4(Ω·m)
Initial value: 12.9%	70.0/0.5	200.0/0.5	40.0/5	60.0
LM (SPIC): 5.4%	67.1/0.8	198.9/0.6	39.8/3.5	60.3
TR (SPICW): 6.1%	45.1/0.6	161.3/0.9	46.5/12.0	97.3
LM (SPICW): 6.0%	50.6/0.6	199.9/0.7	46.5/11.9	96.4

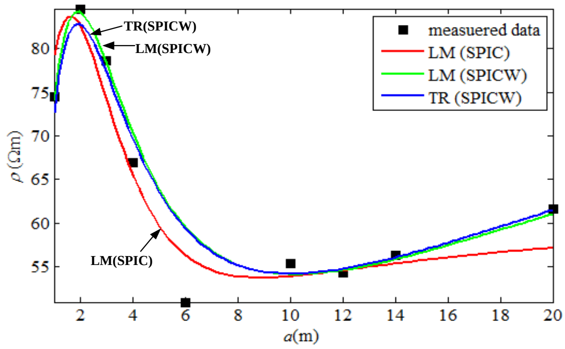

Fig.4. Results of SPIC and SPICW.

VI. CONCLUSION

Soil parameters inversion with constraints has been proposed to avoid unreasonable results and improve confidence of top and deep resistivity. Levenberg–Marquardt method and trust region method are recommended for earth parameter inversion with constraints. But the examples showed that even with constrained optimization methods, sometimes the grounding parameters are affected by the inversed results if the probe spacing is not proper organized. In order to precisely approximate the ρ−a curve by Wenner arrangement, the proper ratio of ascending order probe spacing could be 1:1.5 approximately to get dense enough measured points. Numerical analysis showed that the presented probe spacing configuration can sample the curve precisely and it is a versatile method for all kinds of horizontal multilayer earths.

REFERENCES

[1] IEEE Guide for Measuring Earth Resistivity, Ground Impedance, and Earth Surface Potentials of a Ground System, IEEE Std. 81–2012, 2012.
[2] IEEE Guide for Safety in AC Substation Grounding, IEEE Standard 80–2000, 2000.
[3] J. Ma, F. Dawalibi and W.Daily. "Analysis of grounding systems in soils with hemispherical layering". IEEE Trans. Power Del. ,vol. 8, no. 4, pp. 1773–1781, Oct, 1993.
[4] J. Ma and F. Dawalibi. "Analysis of grounding systems in soils with cylindrical soil volumes." IEEE Trans. Power Del. ,vol. 15, no. 3, pp. 913–918, Jul, 2000,.
[5] J. Ma and F. Dawalibi. "Analysis of grounding systems in soils with finite volumes of different resistivities". IEEE Trans. PowerDel.vol. 17, no. 2, pp. 596 – 602, Apr, 2002.
[6] Y. Chow, J. Yang and K. Srivastava, "Complex images of aground electrode in layered soil," J. Appl. Phys., vol. 71, pp. 569–574,1992.
[7] Z. Li, W. Chen and J. Fan,"A novel mathematical modeling of grounding system buried in multilayer Earth," IEEE Trans. Power Del., 21(3), 1267−1272, Jul. 2006.
[8] F. Wenner. "Method of measuring earth resistivity," Bull. Nat. Bureau Std., Washington D.C., vol. 12, 1916.

[9] B. Zhang, X. Cui and L. Li. "Parameter estimation of horizontal multilayer earth by complex image method," IEEE Trans. Power Del. ,vol. 20, no. 2, pt. 2, pp. 1394–1401, Apr. 2005.

[10] I. Gonos and I. Stathopulos. "Estimation of multilayer soil parameters using genetic algorithms," IEEE Trans. Power Del., vol. 20,no. 1, pp. 100–106, Jan. 2005.

[11] E. Sunde. Earth Conduction Effects in Transmission Systems. New York: Dover, 1968.

[12] W. Calixto, L. Neto and M. Wu. "Parameters estimation of a horizontal multilayer soil using genetic algorithm," IEEE Trans. Power Del., vol. 25,no. 3, pp. 1250–1257, Jul. 2010.

[13] W. Calixto, A. Coimbra and B. Alvarenga. "3−D Soil Stratification Methodology for Geoelectrical Prospection," IEEE Trans. Power Del., vol. 27,no. 3, pp. 1636–1643, Jul. 2012.

[14] H. Seedher and J. Arora. "Estimation of two layer soil parameters using finite Wenner resistivity expressions," IEEE Trans. Power Del., vol. 7, pp. 1213–1217, Jul. 1992.

[15] Y. Chow. "Surface voltages and resistance of grounding systems of grid and rods in two−layer earth by the rapid Galerkin's moment method," IEEE Trans. Power Del., vol. 12, pp. 179–185, Jan. 1997.

[16] P. Lagace, J. Fortin and E. D. Crainic. "Interpretation of resistivity sounding measurement in N−layer soil using electrostatic images," IEEE Trans. Power Del., vol. 11, no. 3, pp. 1349–1354, Jul. 1996.

[17] P.Lagace, M. Vuong and M. Lefebvre. "Multilayer resistivity interpretation and error estimation using electrostatic images," IEEE Trans. Power Del., vol. 21, no. 4, pp. 1954–1960, Oct. 2006.

[18] T. Takahashi and T. Kawase. "Analysis of apparent resistivity in a multi−layer earth structure," IEEE Trans. Power Del., vol. 5, pp. 604–612, Apr.1990.

[19] J. Alamo, "A comparison among eight different techniques to achieve an optimum estimation of electrical grounding parameters in two−layered earth," IEEE Trans. Power Del., vol. 8, pp. 1890–1899, Oct. 1993.

[20] R. Mead and J.A. Nelder. "A simplex method for function minimization," Computer. J, vol.7, no.1, pp. 308−313, 1965.

[21] Low frequency analysis of conductor networks–user's manual for computer program MALT, Safe Engineering Services & Technologies Ltd, Montreal, Canada, 1999.

[22] G. O. Young, "Synthetic structure of industrial plastics (Book style with paper title and editor)," in Plastics, 2nd ed. vol. 3, J. Peters, Ed. New York: McGraw-Hill, 1964, pp. 15–64.

ISBN: 978-988-19252-0-6
ISSN: 2078-0958 (Print); ISSN: 2078-0966 (Online)